

Pavement Geometry in Microscale Urban Heat Islands

Sushobhan Sen, Graduate Research Assistant, University of Illinois at Urbana-Champaign
Jeffery Roesler, Professor & Associate Head, University of Illinois at Urbana-Champaign

Paper prepared for presentation
at the **CLIMATE – HOW IS YOUR JURISDICTION/ORGANIZATION RESPONDING** Session

of the 2017 Conference of the
Transportation Association of Canada
St. John's, NL

Funding for this research was provided by the US Department of Transportation through the University
Transportation Center for Highway Pavement Preservation (UTCHPP) at Michigan State University

ABSTRACT

The Urban Heat Island (UHI) phenomenon has been observed in hundreds of cities across the world, which have been shown to be warmer than adjacent rural areas. Within a city however, the heterogeneity and large number of variables acting simultaneously can make it difficult to understand how UHI develops at a microscale. Urban roads can have different materials and layered structures (collectively called ‘pavement geometry’) in a city and can also be positioned differently with respect to the urban form. A three-factorial analysis was performed using an uncoupled pavement-3D urban canyon model to investigate how pavement geometry, urban form, and meteorological conditions affect microscale UHI. Representative temperature data from Chicago, USA was obtained and the UHI in a simulated urban area was evaluated for the warmest and coldest hours of the year. During the warmest hour, urban form and pavement geometry could increase the microscale UHI by an additional 3°C at distinct spatial locations. Whereas, during the coldest hour which included no sunlight, urban form played a more significant role to locally increasing the UHI by 1 to 1.5°C. Additionally, in closed urban canyons with constricted wind flows, pavement geometry has a particularly important role to play, whereas in more open spaces, the wind flow pattern affects the UHI. Ultimately, multiple microscale UHI case studies are recommended for individual cities to factor in the large number of site-specific variables.

INTRODUCTION

The continuing growth of cities across the world brings with it several environmental challenges. Among them is the Urban Heat Island (UHI), a phenomenon in which urban areas sustain a higher temperature than adjacent rural areas. UHI has been observed in several cities across the world (1,2,3,4) and has been found to be increasing over time with increasing urbanization (5). The UHI in Chicago was one of the reasons attributed for the death of over 500 people in the 1995 heat wave (6), and has been shown to increase average water consumption in Phoenix, Arizona (7). The UHI intensity (ΔT_{ur}) is defined as the difference between the urban and rural temperature, and can be measured at any height. Specifically, the UHI intensity at canopy height (about 2 m above ground level) is most relevant, as it is at this height that most outdoor human activity takes place. This intensity has been observed to vary from less than 1°C to over 10°C, and varies with time and location, both geographically and within a city (8,9). Furthermore, UHI can be studied at a mesoscale, covering entire cities, or at microscale, covering only some parts of a city. In this study, microscale UHI was of interest as it allows pavement engineers to assess the impact of individual roads, including its layered structure, construction materials, and geometry, on the surrounding urban environment.

UHI is caused by several factors, including anthropogenic heat, increased absorption of solar radiation by construction materials, and the loss of natural vegetation and evapotranspiration (10,11). Man-made surfaces made of construction materials can be broadly classified into three categories in cities: roads, roofs, and walls. Several past studies have examined the role played by pavements in the UHI (12,13) and ways to mitigate those effects using ‘cool pavements’ with a high surface albedo (14) as well as by modifying the pavement structure (15). However, these studies consider only specific materials and pavement structures, and discuss only their impact on a city when applied uniformly. Whereas, in practice, cities consist of many different types of pavements – both in terms of structure and materials – whose aggregate impact on cities has not been sufficiently examined. Furthermore, even pavements made of the same material have different thermal properties depending on their age and exposure to the environment (16,17) and the varying impacts of new and aged pavements have not been adequately studied. In this paper, the material, structure, and relative position of pavements are collectively called ‘pavement geometry’ for brevity.

In addition to pavement geometry, the shape and size of the surrounding buildings with respect to the road (collectively called the urban form) has also shown to affect UHI intensity (18,19,20,21,22,23) by altering wind flow patterns and developing vortices in urban canyons, which in turn affects convective cooling and temperature advection (24,11). Because these wind flow patterns tend to be highly non-linear, there is no simple relationship between canopy temperature and surface temperature of roads in an urban environment. Thus, it becomes necessary to use principles of Computational Fluid Dynamics (CFD) to examine the combined impact of pavement geometry and urban form, as well as meteorological factors like wind speed and solar radiation.

Previous studies (20,18,21) have examined either the effect of uniform pavement geometries on different urban forms, or varying pavement geometries for a single urban form (15). However, a more practical case would be to vary both simultaneously. In this study, the authors extend a previous 2D study (21) to a 3D uncoupled pavement-urban canyon model with varying urban form and pavement geometries. This analysis framework allows researchers, transportation engineers, and urban planners to make project level decisions to mitigate UHI.

METHODOLOGY

Scope

This study was a three-factor analysis of the impact of pavement geometry, urban form, and time of day on the average canopy-level temperature, defined as 2 m above ground level, in a simulated 3D urban environment in Chicago, USA. Chicago has a northern, continental climate with cold winters and hot and humid summers. Pavement geometry was varied by using three different types of pavements, with age of the pavements being a factor in the analysis. Urban form was varied by considering two different building heights: 5 m and 20 m. Finally, the time of day was varied by choosing the warmest and coldest hours from a statistically representative Typical Meteorological Year (TMY) (25) following the approach in a previous work by the authors (21). Each of these factors is discussed in detail in the following sub-sections.

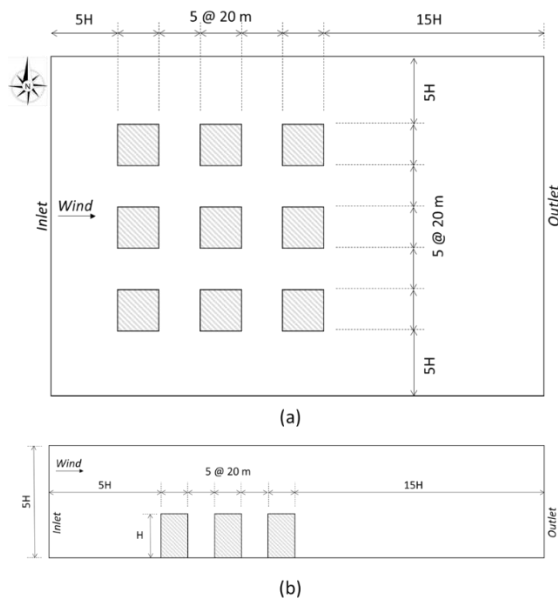


Figure 1: Domain of study in (a) Plan view and (b) Profile view

Urban Form

A small urban segment consisting of a 5 x 5 grid of buildings and roads was chosen to represent the urban form, which is shown in plan and profile views in Figure 1. The width of the roads and buildings was fixed at 20 m,

which represents an average building surrounded by a road with 2 lanes and shoulders. This area, described as 'the city,' is the region of interest within which temperatures will be examined after they are computed for the entire domain. Surrounding the city are wider roads that lead into the city (described in greater detail in the next section). The assumption here is that the city is surrounded by roads connecting to other cities, beyond which is vegetation, which is not explicitly modeled.

The size of these roads outside the city are selected based on the building height, H , to ensure that the inlet and outlet for wind flow (also shown in Figure 1) are far away enough from the city so as not to affect the results. These dimensions were chosen from best practice guidelines for urban modeling (26), with the inlet at a distance of $5H$ from the city, the outlet at $15H$, and side and top walls at $5H$. Thus, for a higher building height H , the size of the domain increases in both the horizontal and vertical directions, although the horizontal extent of the city remains fixed at 100 x 100 m.

To examine the effect of different urban forms, two values of H were used: 5 m and 20 m. The former represents an area with single story buildings, while the latter represents multi-story buildings. The former represents suburban areas, with 5 m building heights, while the latter (20 m) represents a central business district.

Pavement Geometry

Urban roads can typically be classified into three categories: arterials, collectors, and local streets. Arterials carry the largest volume between major city districts or between cities; collectors channel traffic from local streets to arterials and carry a volume of traffic in between the two; and local streets provide door-to-door connectivity with lower traffic volumes. A typical city has all three types of roads with collectors and local streets being the most common types inside the city. Furthermore, these pavements may be new or significantly aged, which affects their thermal and optical properties such as albedo (27,16).

For this study, the assumed distribution of these roads is shown in Figure 2. Each of these was modeled as either a new road, or an aged road. Arterial roads were assumed to surround the city segment, as would be the case for a small segment of a city. Inside the city, West-East roads in the direction of wind flow were assumed to be collectors for this analysis. The collectors further branch out into local streets in a North-South direction, and are perpendicular to the direction of flow. A typical pavement structure for each type of road is as follows:

- (a) Arterials were assumed to have a 200 mm layer of concrete over 100 mm cement stabilized base on top of natural subgrade.
- (b) Collectors were assumed to have a 200 mm layer of concrete over a 200 mm granular base on top of natural subgrade.
- (c) Local streets were assumed to have a 100 mm layer of HMA on top of a 200 mm granular base placed on a natural subgrade.

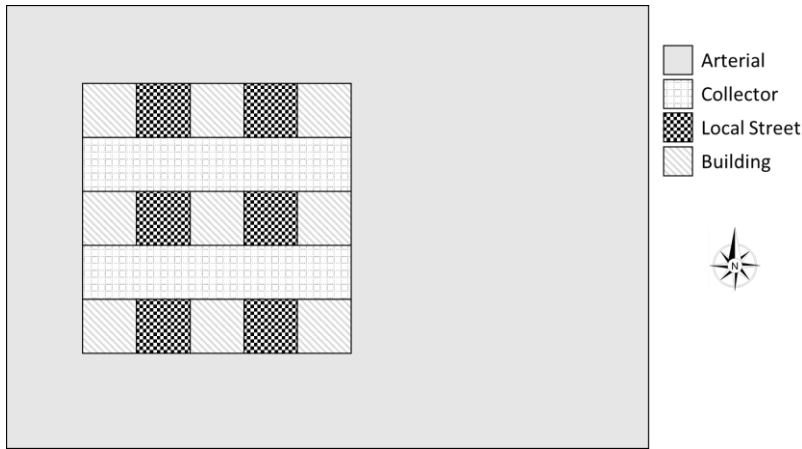


Figure 2: Distribution of roads in the domain

The thermal properties of each of these layers varies and are shown in Table 1. The albedo for new and aged pavements is based on typical values for asphalt and concrete listed in literature (16,27), while other thermal properties, which were assumed to not vary with age, were taken from the default values in the Mechanistic Empirical Pavement Design Guide (MEPDG) (28). The thermal properties of granular layers and the subgrade are a function of their moisture content and are calculated internally during the simulation.

Table 1: Thermal and Optical Properties of Pavements

Property	Arterials	Collectors	Local Streets
Albedo of new pavements	0.40	0.40	0.05
Albedo of aged pavements	0.20	0.20	0.20
Surface emissivity	0.93	0.93	0.93
Surface layer conductivity (W/mK)	2.16	2.16	1.16
Surface layer specific heat capacity (kJ/kgK)	1.17	1.17	0.96
Surface layer density (kg/m ³)	2403	2403	2403
Base layer conductivity (W/mK)	2.16	IC	IC
Base layer specific heat capacity (kJ/kgK)	1.17	IC	IC
Base layer density (kg/m ³)	2403	IC	IC

Properties of subgrade	IC
------------------------	----

IC = Internally Calculated

Weather Data

As discussed in (21), selecting weather data for a UHI study can be difficult. Most studies use an arbitrary ‘warm’ day of the year, which does not consider the representativeness of that day to average meteorological data. Therefore, following reference (21), representative data from Chicago from the Typical Meteorological Year (TMY) Series 3, covering the weather data from 1961-1990 (25) was used. The TMY weather files consist of hourly data from months that show the least deviation in air temperature from the average over the 30-year period. From this data, the warmest and coldest hours of the year were found to be July 19, 3:00 PM (air temperature of 35°C) and January 7, 7:00 AM (air temperature of -22.8°C) respectively, and the analysis was performed for these two hours. For the coldest hour, the sun has not risen at this time.

An important meteorological variable is the wind speed and direction. The TMY data is only built for air temperature, and does not provide a way to obtain a representative wind speed. However, high wind speeds are known to reduce the UHI intensity (20). Therefore, to focus on the effect of pavement geometry and urban form, a low wind speed of 2 m/s at a height of 1.5 m (which is typically the height at which wind speed is measured) is used. The wind is assumed to blow from the west parallel to the collectors and perpendicular to the local streets.

Pavement and Building Thermal Modeling

For simulating the UHI, an uncoupled pavement-urban canyon model developed in a previous study (21) was expanded to three dimensions. In this scheme, the surface temperature of the pavements was evaluated using a 1D heat transfer model, ILLI-THERM, developed previously by the authors (15). The ILLI-THERM program was used to evaluate the hourly surface temperature for the TMY year. The pavement temperature at the hours of maximum and minimum air temperature described in the previous sub-section were used as inputs to the urban canyon CFD model discussed in the next sub-section.

Aside from pavements, buildings also contribute to the UHI. These were modeled in another separate 1D model. It was assumed that the walls and roofs were each 100 mm thick concrete. The CFD solver, ANSYS FLUENT (29), automatically traces the direction of sunlight and evaluates the surface temperature of walls and roofs, considering convective and radiative heat transfer. The thermal properties were kept constant across all the simulations so that any differences would be purely because of the differences in pavement geometry and urban form.

3D CFD Analysis

The urban canyon was solved using the 3D CFD solver, ANSYS FLUENT (29). First, the domain in Figure 1 was meshed to discretize the problem. Because of computational costs, a very fine mesh was not possible; instead, a mesh size of 2 m was used in the city, with 10 m outside of it. A mesh convergence study showed that this adequately resolved the solution of interest i.e., the wind and temperature fields at canopy height in the city. Furthermore, with a road width of 20 m, the finer mesh ensured 10 x 10 grid points in the urban canyon, which is sufficient to capture bulk properties, such as average wind speed and average temperature at the canopy height.

The inlet wind direction was assumed to be from the west, with a magnitude of 2 m/s at 1.5 m height. The inlet wind profile $u(z)$ was modeled as a logarithmic profile, as shown in Equation 1 below, based on (30), which is a semi-empirical representation of a fully developed atmospheric boundary layer. Here, z represents the height above the ground, z_0 is the roughness length below which the wind speed was taken to be zero, u_* is the friction velocity, and κ is the von Karman constant.

$$\frac{u(z)}{u_*} = \frac{1}{\kappa} \log\left(\frac{z}{z_0}\right) \quad (1)$$

Here, roughness length z_0 was taken to be 0.0002 m based on the Davenport Roughness Classification (31). This is used to model the upstream surface conditions that are not explicitly modeled. Based on Equation 1, the inlet wind speed at canopy height ($z = 2$ m) is about 2.06 m/s.

Unlike wind speed, there is no suitable temperature profile for the inlet. Instead, the far field air temperature from the TMY data for the corresponding hour of analysis was imposed as a uniform profile on the inlet; this would be the air temperature if the localized effects of the buildings and pavements were not present. The outlet was modeled as a pressure-outlet with the same temperature profile as the inlet, while the lateral and top walls were set to symmetry conditions, like the previous study (21) where the model was developed. The temperature of the roads was fixed to those evaluated by the ILLI-THERM model, while those of the building walls and roofs were calculated in a separate model by the solver, as discussed previously.

The CFD solver solved the complete Navier-Stokes Equations as well as the Energy Equation with a Realizable $k - \epsilon$ turbulence model and standard wall functions (29). As the wind speeds were much lower than the speed of sound, a pressure-based solver was used, while buoyancy was ignored to lower computational costs. In all cases, the model was run to 2,000 iterations, at the end of which scaled residuals were found to be in the range of $10^{-2} - 10^{-4}$, except for temperature, which was of the order of 10^{-6} .

From the 3D wind speed and temperature fields, the 2D fields at canopy height were extracted. Canyons were evaluated in two directions: parallel and perpendicular to the wind. In each direction, two axes were chosen along which the data was extracted, as shown in Figure 3. Along each axis, results within five distinct canyons (A, B, C, D, and E in Figure 3(a) parallel to the wind, and F, G, H, I, and J in Figure 3(b) perpendicular to the wind) were averaged to obtain the average wind speed and temperature at canopy height for each canyon. These axes were chosen to be such that the canyons would be equidistant from the bounding walls and thus be affected by them equally. Canyons B and D along axes 1 and 2, and canyons G and I along axes 3 and 4 are intersections.

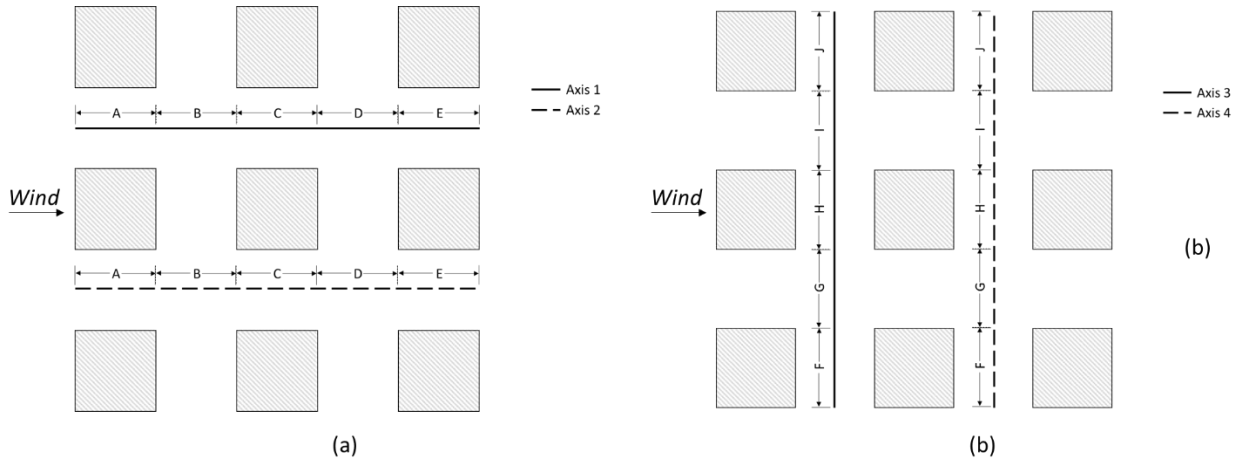


Figure 3 Axes (1 to 4) and canyons (A to E) along which temperature and wind fields were averaged (a) parallel to wind and (b) perpendicular to wind.

RESULTS AND DISCUSSION

Surface Temperatures

The surface temperatures of each of the pavement geometries was evaluated using ILLI-THERM and the results shown in Figure 4(a) and (b) for new and aged pavements, respectively. As expected, the surface temperatures were found to be higher than the air temperature during the warmest as well as coldest hours of the typical year

for all cases. For new pavements in the warmest hour, local streets were found to have a higher temperature than collectors because of their lower albedo, while arterials had a lower temperature than collectors because of heat energy transmitted and stored in the stabilized base layer of the arterials relative to the granular base of the collectors (15). The trend was the opposite during the coldest hour, with arterials having a higher temperature than collectors, which had a higher temperature than local streets. This behavior is because the heat stored in the stabilized base of the arterials is gradually released to the surface during the night, keeping it warmer than the cases with granular bases, which quickly release the heat because of their lower thermal inertia (15). For aged pavements, the albedo was the same for all the roads, but the surface temperature still followed the same pattern during both the warmest and coldest hours, although the magnitude of the differences was lower. The differences in surface temperature was again attributed to the thermal properties of the pavement structure.

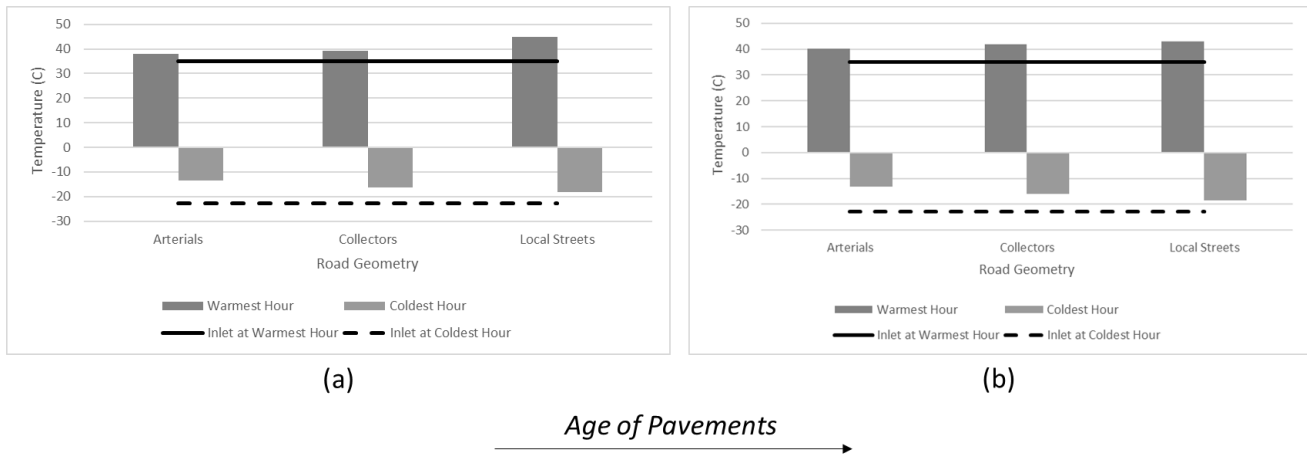


Figure 4: Surface temperatures for (a) new pavements and (b) aged pavements, as well as inlet air temperatures at warmest and coldest hours.

Wind Speeds

The wind speed for each case was evaluated by the CFD solver and the average wind speed at canopy height in each canyon (A to E parallel to the wind, and F to J perpendicular), as described in Figure 3, are shown in Figure 5 and Figure 6, respectively, for new pavements. The corresponding results for aged pavements are shown in Figure 7 and Figure 8, respectively.

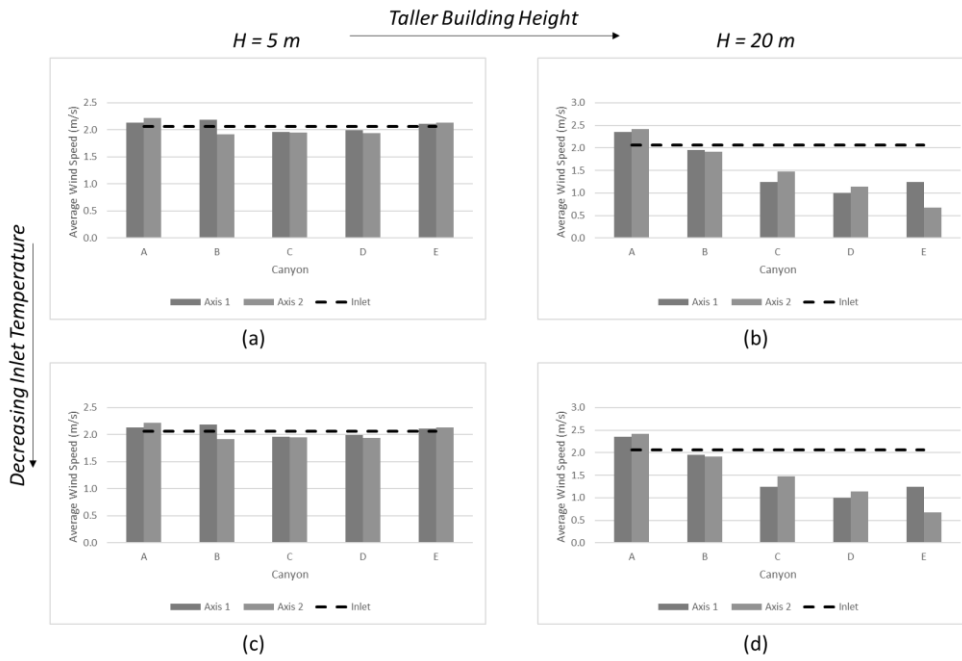


Figure 5: Average canopy height wind speed in each canyon parallel to the direction of flow for (a) 5 m building height in the warmest hour (b) 20 m building height in the warmest hour (c) 5 m building height in the coldest hour and (d) 20 m building height in the coldest hour with new pavements.

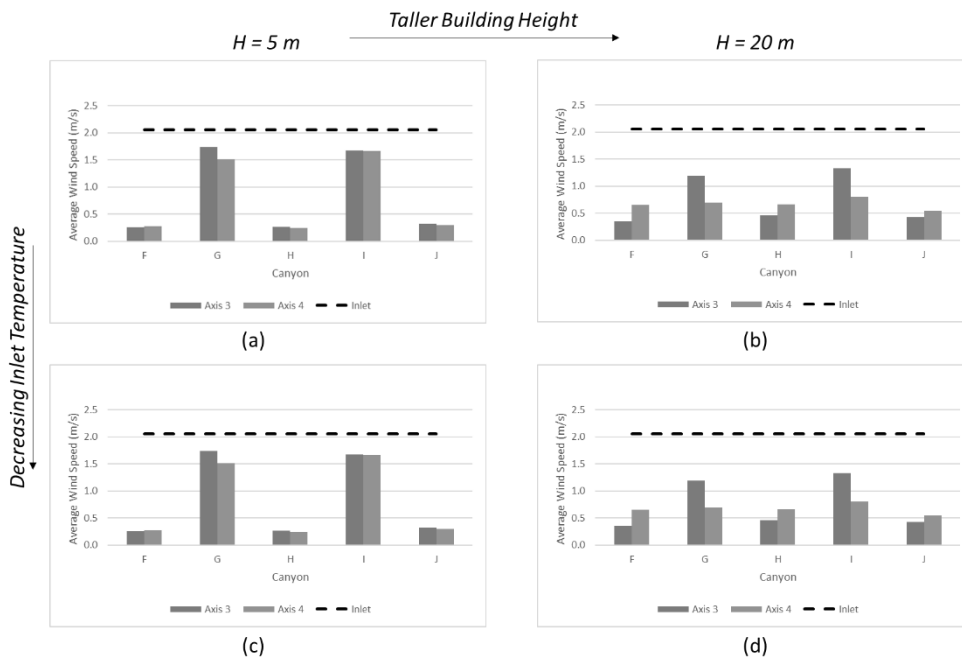


Figure 6: Average canopy height wind speed in each canyon perpendicular to the direction of flow (a) 5 m building height in the warmest hour (b) 20 m building height in the warmest hour (c) 5 m building height in the coldest hour and (d) 20 m building height in the coldest hour with new pavements.

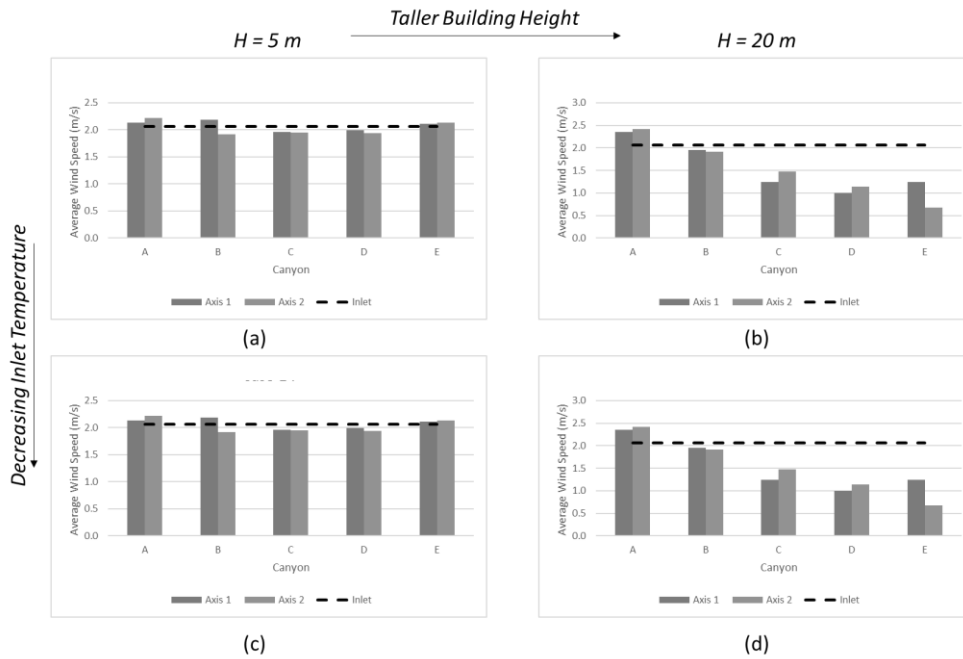


Figure 7: Average canopy height wind speed in each canyon parallel to the direction of flow (a) 5 m building height in the warmest hour (b) 20 m building height in the warmest hour (c) 5 m building height in the coldest hour and (d) 20 m building height in the coldest hour with aged pavements.

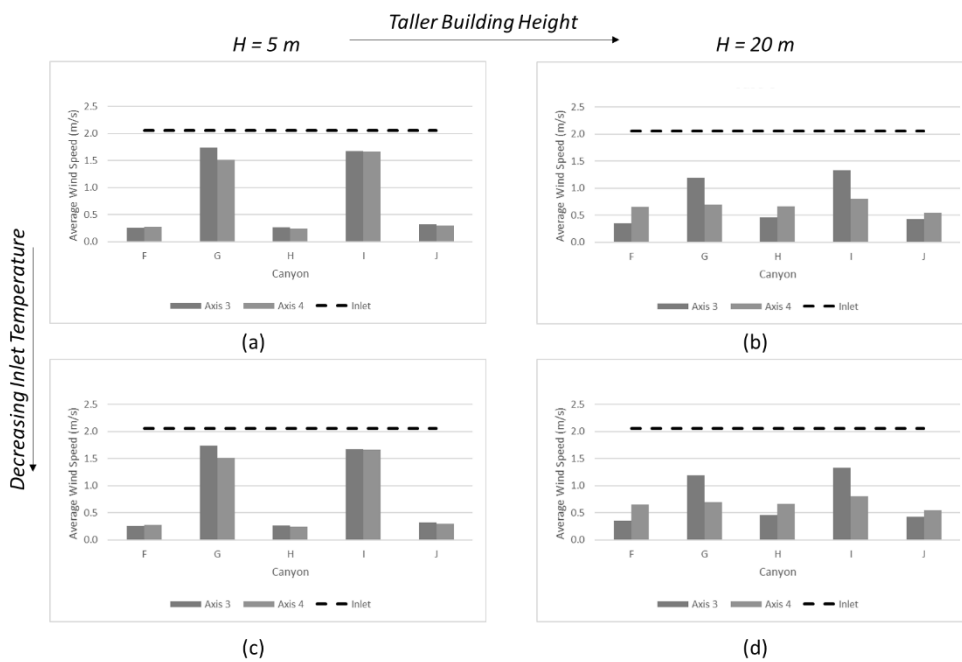


Figure 8: Average canopy height wind speed in each canyon perpendicular to the direction of flow (a) 5 m building height in the warmest hour (b) 20 m building height in the warmest hour (c) 5 m building height in the coldest hour and (d) 20 m building height in the coldest hour with aged pavements.

In the microscale domain analyzed, wind speed is not affected by the inlet temperature or pavement geometry (including pavement structure, geometry, and age), but is strongly affected by the urban form. Thus, for a given inlet temperature and urban form in Figure 5 or Figure 6 (new pavements), the corresponding wind speed for the same inlet temperature and urban form in Figure 7 or Figure 8 (aged pavements), respectively, is

approximately same. Whereas, for a fixed pavement geometry and inlet temperature, the wind speed decreases in the direction of flow with increasing building height, e.g., see Figure 5(a) and (b).

For the cases with 5 m building height parallel to the wind flow (Figure 5 and Figure 7), the wind speed does not vary significantly from the far field value set at the inlet, indicating that low buildings do not change the wind flow pattern much. Whereas for the cases with 20 m building height, wind speed decreases significantly from being a little higher than the inlet value in Canyon A to only about half of that in Canyon E, indicating that the taller buildings constrict the wind flow. The results for corresponding canyons between axes 1 and 2 are slightly different from each other and are expected to be the same because of the domain symmetry assumption. This difference comes from numerical error, which can be minimized by using a finer mesh. However, as this requires more computational resources, these results with small errors were accepted for this study.

The results are quite different perpendicular to the wind flow (Figure 6 and Figure 8). Here, two distinct patterns can be seen: Canyons F, H, and J show a lower wind speed, while G and I show a higher speed. This can be explained by considering Figure 3(b). Canyons F, H, and J are constricted by buildings on two sides, whereas G and I are part of an intersection and are not constricted. In other words, G and I are directly in the path of the incoming wind, where F, H, and J are shielded by the buildings. Consequently, G and I show a higher wind speed than F, H, and J; the wind speed in F, H, and J are a result of the formation of local vortices within the canyons (24), while it is due to the wind flowing from the inlet for G and I. The difference between these two patterns is higher for cases with 5 m building height and lower for the 20 m cases, once again indicating that the taller buildings constrict the wind flow. Furthermore, axes 3 and 4 show different results for the corresponding canyons, but this is expected as the wind speed dissipates from upstream (axis 3) to downstream (axis 4).

Temperatures

Similar to wind speed, the average temperature at canopy height parallel and perpendicular to the wind flow is shown in Figure 9 and Figure 10, respectively, for new pavements, and Figure 11 and Figure 12, respectively, for aged pavements. These can be analyzed in several ways, keeping in mind that both wind field and pavement surface temperatures affect the result. As discussed previously in Figure 4 at the warmest hour for both new and aged pavements, the arterials upstream and downstream of the city have a lower surface temperature than the collectors and local streets; and at the coldest hour, arterials have a higher surface temperature than the collectors/local streets. This will become important in understanding the calculated air temperatures in the canyons.

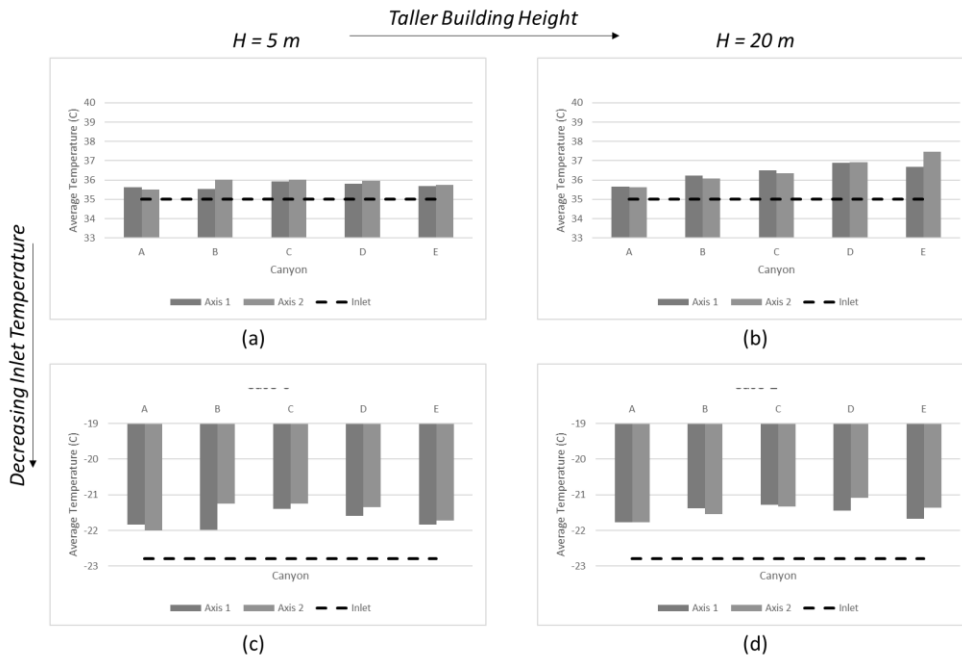


Figure 9: Average canopy height temperature in each canyon parallel to the direction of flow for (a) 5 m building height in the warmest hour (b) 20 m building height in the warmest hour (c) 5 m building height in the coldest hour and (d) 20 m building height in the coldest hour with new pavements.

First, consider only the new pavements. Parallel to the wind flow (Figure 9a), for the warmest hour under the 5 m building height case, canyons B, C, and D have approximately the same temperature, about 1°C higher than the inlet value, while A and E have a slightly lower temperature (about 0.5 to 0.75°C greater than the inlet value) because of the influence of the cooler arterials near them, as well as the higher wind speed upstream of canyon A. At the same hour with 20 m building height (Figure 9b), there is a clearly increasing temperature trend along the two axes, from canyon A to canyon E, with the temperature increasing from 0.5°C to 2.5°C above the inlet value, which correlates with the decreasing wind speed observed for the same case in Figure 5(b). Since all the canyons along axes 1 and 2 are of the pavement geometry (arterials), wind speed and urban form have the most influence on the canopy height air temperature. Furthermore, between axes 1 and 2 for corresponding canyons, the results are slightly different because of numerical errors as discussed previously.

For the coldest hour, there is no sunlight and the surface temperature depends on the amount of heat stored in the pavement structure and released from the previous day. In Figure 9(c) and (d), the case with 5 m building height has, in general, a lower temperature than the 20 m case, of an average magnitude of 0.5°C, due to the higher wind speed in the former. Interestingly, in both cases, canyons A and E have a slightly lower temperature than canyons B, C, and D, despite the influence of the warmer arterials (Figure 4). The most likely reason for this is the heat emitted from the buildings, which affects the inner canyons (B, C, and D) more than the outer ones (A and E), as well as the higher wind speed upstream of A.

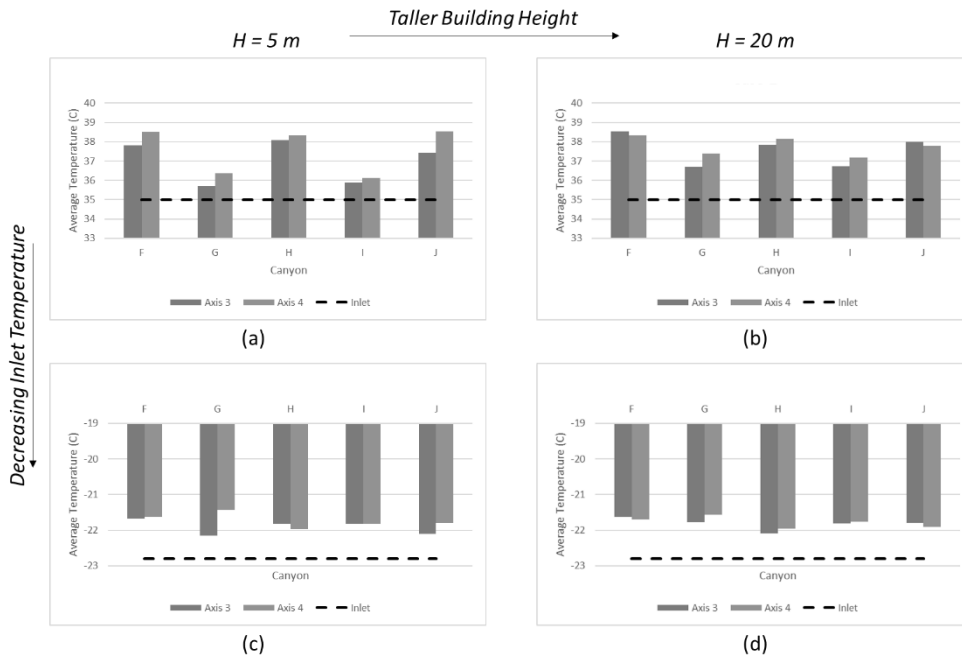


Figure 10: Average canopy height temperature in each canyon perpendicular to the direction of flow for (a) 5 m building height in the warmest hour (b) 20 m building height in the warmest hour (c) 5 m building height in the coldest hour and (d) 20 m building height in the coldest hour with new pavements.

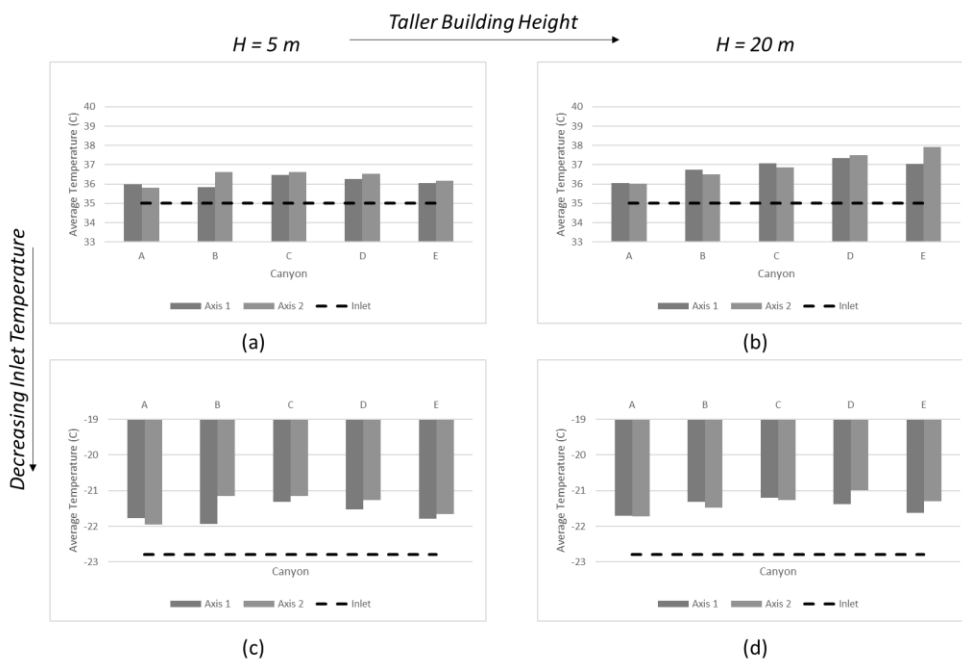


Figure 11: Average canopy height temperature in each canyon parallel to the direction of flow for (a) 5 m building height in the warmest hour (b) 20 m building height in the warmest hour (c) 5 m building height in the coldest hour and (d) 20 m building height in the coldest hour with aged pavements.

Still considering only new pavements, but this time perpendicular to the wind flow in Figure 10(a) and (b), during the warmest hour, two distinct temperature patterns can be observed: canyons F, H, and J have a higher temperature than G and I. Once again, this correlates with the two patterns seen in the wind flow for the same case in Figure 6(a) and (b). Furthermore, canyons F, H, and J correspond to the low-albedo local streets that have a higher surface temperature, whereas G and I correspond to the collectors with a low surface

temperature. This further increases the air temperature to about 3°C above the inlet value for the canyons above the local streets and about 1°C above the collectors.

During the coldest hour, however, in Figure 10(c) and (d), for the 5 m building height case, there is not much difference in the temperatures despite the significant difference in wind speed and pavement structure, with the temperatures being about 1 to 1.5°C warmer than the inlet. A similar trend is observed in the 20 m case. Parallel to the wind flow, canyons of higher wind speed show a lower average air temperature at canopy height as the warmer air is simply advected downstream faster, but perpendicular to it, that is the not case as the local air flow is restricted to within the canyon itself due to the formation of vortices in them (24,21). In this study, a West-East wind was considered; however, the direction and speed of the wind changes continuously because of changes in the atmosphere, and those changes directly impact the UHI, as canyons that were previously either parallel or perpendicular to the wind, can have both parallel and perpendicular components when the wind direction changes. This illustrates the need for further modeling taking wind speed and direction into account.

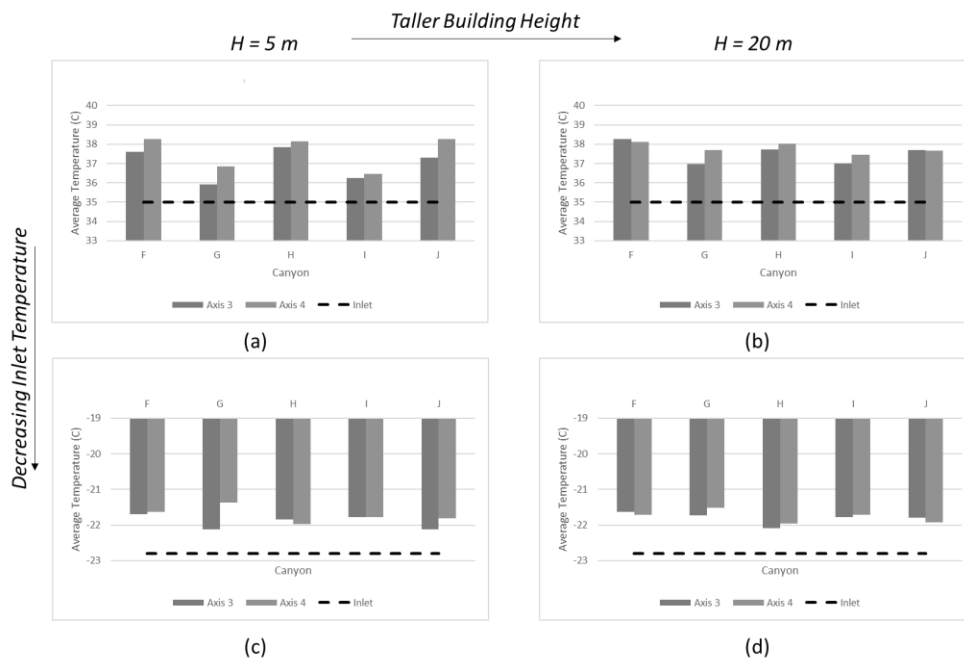


Figure 12: Average canyon height temperature in each canyon perpendicular to the direction of flow for (a) 5 m building height in the warmest hour (b) 20 m building height in the warmest hour (c) 5 m building height in the coldest hour and (d) 20 m building height in the coldest hour with aged pavements.

For aged pavements, the trends in the results are the same as for the new pavements, but the magnitude is slightly different due to the lower albedo for the arterials and collectors, and higher for the local streets. In general, albedo does not have much of an effect for the coldest hour due to the absence of sunlight, and pavement structure and urban form have the greatest effect.

Design Implications

From the preceding results, it becomes clear that predicting the microscale UHI in parts of a city can be quite complicated. Pavement geometry (including age of the pavements), urban form, and meteorological conditions each contribute to the development of the local microscale UHI, which can be less than 0.5°C to over 3°C higher than the far field value set at the inlet during the warmest hour of the year, and 1 to 1.5°C higher during the coldest hour.

During the warmest hour of the typical meteorological year, when the aim is to lower the canopy layer air temperature, urban form has been shown to mitigate UHI. Low and more open urban forms allow for higher wind flows and lower temperatures, while tall and narrow canyons constrict the wind flow and increase the air

temperature. Low albedo pavements that do not store much heat in the sub-surface layers further exacerbate the problem during the day. In contrast, during the coldest hour of the year, urban form primarily controls the temperature by altering the wind flow, with pavement geometry having only a limited effect. Aside from these extremes, it may be desirable to mitigate the average air temperature rather than the extreme values, in which case a full 24-hour analysis must be performed for various cases, which would be very computationally expensive. In addition, the results also depend on wind speed and direction. Furthermore, policymakers may also be interested in modifying the local microclimate to mitigate building energy use, which adds another layer of computational complexity and may provide different results. Thus, for mitigating UHI, civil engineers and city planners need to consider not just building and pavement geometry but also the relative position of the pavement with respect to specific buildings, as well as the wind direction. This is best done through case by case simulations for individual areas in a city, as opposed to general recommendations.

CONCLUSION

Studying UHI at a microscale can be complex given the many variables involved and their heterogeneous distribution in a city. Pavement geometry, urban form, and meteorological conditions all affect UHI simultaneously. Furthermore, results during the warmest hours when UHI is the strongest do not coincide with simulation results during the coldest hours. In this study, a three-factorial test varying pavement geometry, urban form, and meteorological conditions was conducted through an uncoupled pavement-3D urban canyon model using statistically representative weather data from Chicago, USA for the warmest and coldest hour of the year.

Using an uncoupled pavement-urban canyon model, the surface temperature of the pavement depends on its thermal and optical properties as well as the geometry of the sub-surface layers. During the warmest hour of a typical meteorological year, both pavement geometry and urban form increased air temperature in urban canyons, thus further increasing the local, microscale UHI by as much as 3°C. Parallel to the direction of wind flow, this was primarily affected by the urban form, whereas perpendicular to it, both urban form and pavement geometry had an effect. The increase was highest when the wind flow was restricted by tall buildings (in this case, of 20 m height), and when the canyon was perpendicular to the direction of wind flow. Furthermore, wind speed decreased downstream, leading to higher downstream temperatures. Shorter buildings (in this case, of 5 m height) with a more open urban form showed lower increases in UHI due to a smaller decrease in wind speed downstream, although canyons perpendicular to the wind flow still had a higher air temperature than those parallel. Simulation results were similar, though of slightly different magnitude, between new and aged pavements. During the coldest hour, pavement geometry played only a minor role (mainly in the form of heat stored and released by the pavement structure), while urban form played the dominant role by modifying the wind flow patterns. The UHI at the coldest hour increased only 1 to 1.5°C as compared to the corresponding inlet temperature.

Because of the inherent complexity and variability in the problem, it is recommended that case by case simulations are performed, with an initial focus on prevailing wind direction and speed, and also thermal and optical properties of pavements, factors that are typically not considered by transportation engineers. Ultimately, any decision must be based on a clear objective, such as decreasing the peak or average canopy air temperature, or building energy use, and the type of analysis required would follow. Such analyses would provide local solutions to the UHI problem suitable for the unique city conditions.

REFERENCES

1. Tran, H., Uchiyama, D., Ochi, S., Yasuoka, Y. 2006. "Assessment with satellite data of the urban heat island effects in Asian mega cities." In *International Journal of Applied Earth Observation and Geoinformation*, 8(1), pp. 34-48.

2. Arnfield, J.A. 2003. "Two decades of urban climate research: a review of turbulence, exchanges of energy and water, and the urban heat island." In *International Journal of Climatology*, 23(1), pp. 1-26.
3. Peng, S., Piao, S., Ciais, P., Friedlingstein, P., Oettle, C., Breon, FM., et al. 2011. "Surface Urban Heat Island Across 419 Global Big Cities." In *Environmental science & technology*, 46(2), pp. 696-703.
4. Santamouris, M. 2015. "Analyzing the heat island magnitude and characteristics in one hundred Asian and Australian cities and regions." In *Science of the Total Environment*, 512, pp. 582-598.
5. Sone, B. 2007. "Urban and rural temperature trends in proximity to large US cities: 1951–2000." In *International Journal of Climatology*, 27(13), pp. 1801-1807.
6. Changnon, S.A., Kunkel, K.E., Reinke, B.C. 1996. "Impacts and responses to the 1995 heat wave: A call to action." In *Bulletin of the American Meteorological Society*, 77(7), pp. 1497-1506.
7. Aggarwal, RM, Guhathakurta, S, Grossman-Clarke, S, Lathey, V. 2012. "How do variations in Urban Heat Islands in space and time influence household water use? The case of Phoenix, Arizona." In *Water resources research*, 48(6), pp. W06518.
8. Qin, Y, Liang, J, Tan, K, Li, F. 2017. "The amplitude and maximum of daily pavement surface temperature increase linearly with solar absorption." In *Road Materials and Pavement Design*, 18(2), pp. 440-452.
9. Golden, JS, Guthrie, PM, Kaloush, KE, Britter, RE. 2005. "Summertime urban heat island hysteresis lag complexity." In *Proceedings of the Institution of Civil Engineers-Engineering Sustainability*, 158(4), pp. 197-210.
10. Kleerekoper, L, van Esch, M, Salcedo, TB. 2012. "How to make a city climate-proof, addressing the urban heat island effect." In *Resources, Conservation and Recycling*, 6,,: pp. 30-38.
11. Oke, TR. 1982. "The energetic basis of the urban heat island." In *Quarterly Journal of the Royal Meteorological Society*, 108(455), pp. 1-24.
12. Qin, Y. "A review on the development of cool pavements to mitigate urban heat island effect." In *Renewable and Sustainable Energy Reviews*, 52, pp. 445-459.
13. Santamouris, M. 2013. "Using cool pavements as a mitigation strategy to fight urban heat island—A review of the actual developments." In *Renewable and Sustainable Energy Reviews*, 26, pp. 224-240.
14. Yang, J, Wang, ZH, Kaloush, KE. 2015. "Environmental impacts of reflective materials: Is high albedo a 'silver bullet' for mitigating urban heat island?" In *Renewable and Sustainable Energy Reviews*, 47, pp. 830-843.
15. Sen, S, Roesler, JR. 2017. "Microscale heat island characterization of rigid pavements." In *Transportation Research Record: Journal of the Transportation Research Board*, 2639, In Press.

16. Sen, S, Roesler, JR. 2016. "Aging albedo model for asphalt pavement surfaces." In *Journal of Cleaner Production*, 117, pp. 169-175.
17. Levinson, R, Akbari, H. 2002. "Effects of composition and exposure on the solar reflectance." In *Cement and Concrete Research*, 32(11), pp. 1679-1698.
18. Ghaffarianhoseini, A, Berardi, U, Ghaffarianhoseini, A. 2015. "Thermal performance characteristics of unshaded courtyards in hot and humid climates." In *Building and Environment*, 87, pp. 154-168.
19. Yaghoobian, N, Kleissl, J, Paw, U KT. 2014. "An improved three-dimensional simulation of the diurnally varying street-canyon flow." In *Boundary-layer meteorology*, 153(2), pp. 251-276.
20. Gaitani, N, Spanou, A, Saliari, M, Synnefa, A, Vassilakopoulou, K, Papadopoulou, K, et al. 2011. "Improving the microclimate in urban areas: a case study in the centre of Athens." In *Building Services Engineering Research and Technology*, 32(1), pp. 53-41.
21. Sen, S, Roesler, JR. 2017. "An uncoupled pavement-urban canyon model for heat islands." In *Proceedings of the 2017 International Symposium on Pavement Life Cycle Assessment*, Champaign, IL, USA, pp. 111-120.
22. Salata, F, Golasi, I, Vollaro, EL, Bisegna F, Nardecchia F, Coppi, et al. 2015. "Evaluation of Different Urban Microclimate Mitigation Strategies through a PMV Analysis." In *Sustainability*, 7(7), pp. 9012-9030.
23. Moonen, P, Defraeye, T, Dorer, V, Blocken, B, Carmeliet, J. 2012. "Urban Physics: Effect of the microclimate on comfort, health and energy demand." In *Frontiers of Architectural Research*, 1(3), pp. 197-228.
24. Xie, X, Liu, CH, Leung, DYC, Leung, MKH. 2006. "Characteristics of air exchange in a street canyon with ground heating." In *Atmospheric Environment*, 40(33), pp. 6396-6409.
25. NREL. National Solar Radiation Database. [cited 2016 August 1].
http://rredc.nrel.gov/solar/old_data/nsrdb/1991-2005/tmy3/.
26. Franke, J, Hellsten, A, Schlunzen, H, Carissimo, B. 2007. "Best Practice Guideline for the CFD Simulation of Flows in the Urban Environment." COST Action 732: Quality Assurance and Improvement of Microscale Meteorological Models. Hamburg, Germany.
27. Li, H, Harvey, J, Kendall, A. 2013. "Field measurement of albedo for different land cover materials and effects on thermal performance." In *Building and Environment*, 59, pp. 536-546.
28. ARA, Inc. 2004. "Guide for Mechanistic-Empirical Pavement Design of New and Rehabilitated Pavement Structures." Washington, DC. Report No.: National Cooperative Highway Research Program Report 1-37A.
29. ANSYS, Inc. 2009. ANSYS FLUENT v 12.0 Theory Guide.

30. van Hooff, T, Blocken, B. 2010. "On the effect of wind direction and urban surroundings on natural ventilation of a large semi-enclosed stadium." In *Computers & Fluids*, 39(7), pp. 1146-1155.
31. Davenport, A, Grimmond, S, Oke, T, Wieringa, J. 2000. "The revised Davenport roughness classification for cities and sheltered country." In *Proceedings of the 3rd Symposium on Urban Environment*, Davis, CA. American Meteorological Society.